Chaotic advection in compressible helical flow

V. N. Govorukhin,[1] A. Morgulis,[1] V. I. Yudovich,[1] and G. M. Zaslavsky[2,3]
[1]*Department of Mathematics and Mechanics, Rostov State University, 5 Zorge Street, Rostov-na-Donu 344104, Russia*
[2]*Courant Institute of Mathematical Sciences, New York University, 251 Mercer Street, New York, New York 10012*
[3]*Department of Physics, New York University, 2-4 Washington Place, New York, New York 10003*
(Received 11 January 1999)

Compressible helical flow with div $\mathbf{v}\neq 0$ drastically increases the area of chaotic dynamics and mixing properties when the helicity parameter is spatially dependent. We show that the density dependence on the z coordinate can be incorporated in new variables in a way that leads to a Hamiltonian formulation of the system. This permits the application of various important results like the Kolmogorov-Arnold-Moser theory and, particularly, an understanding of why and in which sense the compressible helical flow is ''more chaotic'' than the incompressible one. Simulation demonstrates this property for an analog of the *ABC* flow. An interesting type of the dynamical system with ''dense'' island chains is described. [S1063-651X(99)00109-9]

PACS number(s): 05.45.−a, 03.50.−z, 44.35.+c

I. INTRODUCTION

Helical flow represents a stationary solution of the Euler equation with constant Bernoulli function and it satisfies the equation

$$\mathrm{curl}\mathbf{v}=\kappa\mathbf{v}, \tag{1.1}$$

with a helicity parameter κ which is not necessarily a constant. Interest in Eq. (1.1) emerged long ago and is still active: it is a good model for studying the topology of field lines and advection [1,2], and it has interesting applications in the understanding of turbulence [3,4] and generation of magnetic fields [3,5,2]. It is worth mentioning that replacement of $\mathbf{v}$ by $\mathbf{B}$ leads to the equation for a force-free magnetic field. A particular example of solution of Eq. (1.1), known as *ABC* flow [6,7], was the subject of numerous publications on chaotic advection [8–10] and the fast magnetic dynamo problem [7]. Another type of solution of Eq. (1.1) with generalized symmetry of crystal or quasicrystal type was considered as a source of the emergence of fluid stochastic webs [10,11] for advected particles with anomalous transport along the webs [12,13].

All studies mentioned above considered

$$\kappa=\mathrm{const}, \tag{1.2}$$

which implies the incompressibility condition $\mathrm{div}\,\mathbf{v}=0$. There was a special reason for such restriction because of the Arnold theorem [6]: the topology of field lines is trivial for nonhelical incompressible steady flow as well as for a helical one if $\kappa\neq\mathrm{const}$. The last statement follows immediately from Eq. (1.1) and from the equation for field lines

$$\dot{\mathbf{r}}=\mathbf{v}, \tag{1.3}$$

which coincides with the equation for advected particles, where the dot means derivative with respect to time t. As a consequence of the theorem, trajectories of advected particles are trivial, i.e., Eq. (1.3) is integrable and has a nontrivial integral of motion $\kappa=\kappa(\mathbf{r})$. This explains the motivation for the choice of $\kappa=\mathrm{const}$ when, following the same theorem of Arnold, the dynamics can be nontrivial, i.e., chaotic. The fact that a fast magnetic dynamo can be generated only by chaotic field lines made the case of nonuniform helicity parameter $\kappa=\kappa(\mathbf{r})$ uninteresting, creating a strange situation that was described in detail in [14]: for a typical (from the physical point of view) situation of $\kappa=\kappa(\mathbf{r})$, advected particles always have regular (nonchaotic) dynamics that are nontypical (again, from the physical point of view).

It was proposed in [14] to remove the condition of incompressibility and it was conjectured that in that case solutions of Eq. (1.1) with a typical condition $\kappa=\kappa(\mathbf{r})$ produce a typical (chaotic) dynamics of the advected particles. Here we present a detailed study of the role of compressibility in generating chaotic advection in helical flow. We will also describe a dynamical system with unusual properties, which emerges due to the compressibility of the flow. It is found that the compressibility can increase the mixing property of chaotic advection.

II. HAMILTONIAN EQUATIONS ALONG TRAJECTORIES OF ADVECTION

In this section we show the existence of a Hamiltonian form for the advected particles in compressible helical flow. For a stationary flow

$$\mathrm{div}(\rho\mathbf{v})=0 \tag{2.1}$$

and, without the loss of generality, we can simply set $\rho=\kappa$ [see Eq. (1.1)],

$$\mathrm{div}(\kappa\mathbf{v})=0. \tag{2.2}$$

Consider, for simplicity, the case $\kappa=\kappa(z)$ and rewrite the advection equation (1.3) in the form

$$\frac{d}{d\tau}\mathbf{r}=\kappa\mathbf{v}, \tag{2.3}$$

where a new variable τ is introduced instead of t by the equation

$$\frac{dt}{d\tau}=\kappa(z(t;\kappa_0,y_0,z_0)), \tag{2.4}$$

with initial conditions x_0,y_0,z_0 at $t=0$ and the restriction $\kappa\neq 0, \infty$ at any finite point (x,y,z).

Three equations (2.3) can be written in Hamiltonian form using the condition (2.2). This condition can be considered as a constraint for Eq. (2.3). After excluding the constraint (2.2) and due to the property that the magnitude of $\kappa\mathbf{v}$ is preserved, which follows from Eq. (2.2), we can transform system (2.3) into a Hamiltonian form using an appropriate choice of variables (see, for example, [11]). The choice of Hamiltonian representation is not unique but it does not influence the phase space structure and the physical results for the advection [1].

Let us write

$$\frac{dx}{dz}=\frac{v_x}{v_z}, \quad \frac{dy}{dz}=\frac{v_y}{v_z} \tag{2.5}$$

instead of Eq. (2.3). Let us consider $x=x(z)$, $y=y(z)$ as independent phase-space variables. A change from Eq. (2.5) to a Hamiltonian form of the equations can be done using some general type of transformation from (x,y) to (x,p) variables with

$$p(x,y,z)=\kappa(z)\int_0^y v_z(x,y',z)dy'. \tag{2.6}$$

Let us define

$$H=H(x,p,z)=\kappa(z)\left\{\int_0^y v_x(x,y',z)dy' - \int_0^x v_y(x',0,z)dx'\right\}. \tag{2.7}$$

Then it follows from Eqs. (2.5)–(2.7) that

$$\frac{dx}{dz}=\frac{\partial H}{\partial p}, \quad \frac{dp}{dz}=-\frac{\partial H}{\partial x}, \tag{2.8}$$

i.e., H is the Hamiltonian function for canonically conjugate pair (x,p) and z plays the role of time variable. Again, we consider $x=x(z)$, $p=p(z)$ as independent variables instead of the pair (x,y). The first equation in Eq. (2.8) follows directly from Eq. (2.7) and definition (2.6). To prove the second one, consider the expression

$$\frac{\partial H}{\partial x}=\kappa(z)\left\{\int_0^y \frac{\partial v_x(x,y',z)}{\partial x}dy'-v_y(x,0,z)\right\} \tag{2.9}$$

and use condition (2.2), which gives

$$\begin{aligned}\frac{\partial H}{\partial x}&=-\int_0^y \kappa(z)\frac{\partial v_y(x,y',z)}{\partial y'}dy' \\ &\quad -\int_0^y \frac{\partial}{\partial z}[\kappa(z)v_z(x,y',z)]dy'-\kappa(z)v_y(x,0,z) \\ &=-\kappa(z)v_y(x,y,z)-\int_0^y \frac{\partial}{\partial z}[\kappa(z)v_z(x,y',z)]dz.\end{aligned} \tag{2.10}$$

From Eqs. (2.6) and (2.5) we have

$$\begin{aligned}\frac{dp}{dz}&=\kappa(z)v_z\frac{dy}{dz}+\int_0^y \frac{\partial}{\partial z}[\kappa(z)v_z(x,y',z)]dy' \\ &=\kappa(z)v_y(x,y,z)+\int_0^y \frac{\partial}{\partial z}[\kappa(z)v_z(x,y',z)]dy'.\end{aligned} \tag{2.11}$$

Comparing Eqs. (2.10) and (2.11) proves the second equation (2.8). There are other Hamiltonian representations which may be convenient for different situations depending on the considered flow [11].

The existence of an even local Hamiltonian form for the advection equation (2.3) in the compressible case permits us to apply Hamiltonian dynamics theory. In particular, we can immediately state that a generic three-dimensional helical compressible flow generates advection with chaotic trajectories in analogy to the statement that a Hamiltonian system with $1\frac{1}{2}$ degrees of freedom possesses, typically, chaotic trajectories [1,11]. Moreover, we expect the existence of an infinite number of islands which are isolated from the stochastic sea and which are filled by invariant curves according to the Kolmogorov-Arnold-Moser (KAM) theory. The Hamiltonian type of chaos means also the absence of strange attractors in the presence of compressibility. In addition, in Sec. V we will comment on why the compressibility of the type considered here leads to a ''stronger'' chaos than in the incompressible case.

III. BASIC EQUATIONS

Consider an example of the compressible flow obtained in [14]:

$$\begin{aligned}v_x&=-4\frac{dW}{d\zeta}\sin x-4W\sin y+\epsilon\sin\zeta, \\ v_y&=-4\frac{dW}{d\zeta}\sin y+4W\sin x+\epsilon\cos\zeta, \\ v_z&=4\frac{W}{\kappa}(\cos x+\cos y),\end{aligned} \tag{3.1}$$

where ϵ is a constant, the variable ζ is introduced instead of z by the equation

$$\frac{d\zeta}{dz}=\kappa(z), \tag{3.2}$$

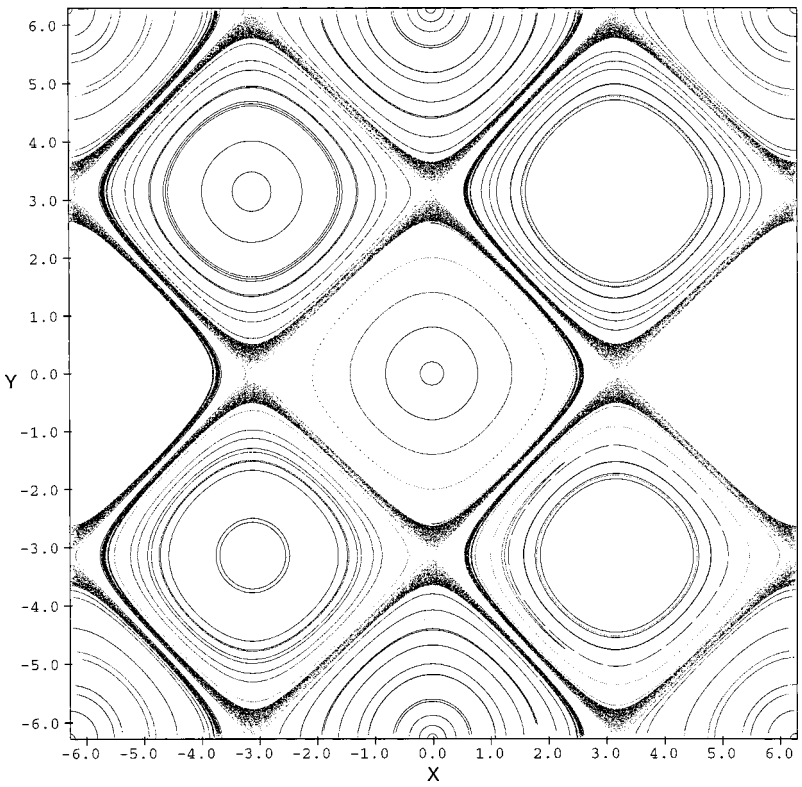

FIG. 1. Poincaré section of trajectories in $z=0$ plane for the *ABC* flow with $\epsilon=0.05$.

and $W=W(\zeta)$ is a solution of the equation

$$W''+(1-1/\kappa^2)W=0. \tag{3.3}$$

For the case of $\kappa=1$ and $W=\text{const}$, the system (3.1) converts to a particular case of the *ABC* flow. We can say that Eq. (3.1) is a compressible analog of the *ABC* flow and refer to it as the *CABC* flow. Field (3.1) satisfies Eq. (1.1) with an arbitrary helicity parameter function $\kappa(z)$.

The advection equation (1.3) that corresponds to Eq. (3.1) can be written as

$$\dot{x}=-4\frac{dW}{d\zeta}\sin x-4W\sin y+\epsilon\sin\zeta,$$

$$\dot{y}=-4\frac{dW}{d\zeta}\sin y+4W\sin x+\epsilon\cos\zeta, \tag{3.4}$$

$$\dot{z}=4\frac{W}{\kappa}(\cos x+\cos y)=\frac{1}{\kappa}\dot{\zeta},$$

where we use the condition (3.2). For the incompressible uniform case ($\kappa=1$, $W=\text{const}$), the system (3.4) is reduced to the *ABC* flow

$$\dot{x}=-4W\sin y+\epsilon\sin z,$$

$$\dot{y}=4W\sin x+\epsilon\cos\zeta, \tag{3.5}$$

$$\dot{z}=4W(\cos x+\cos y).$$

We will consider the nonuniformity of the helicity parameter (and density) in the form

$$\kappa=\kappa(\zeta)=[1+4/\ell^2+6/\ell^2\cosh^2(\zeta/\ell)]^{-1/2}, \tag{3.6}$$

with a characteristic length scale ℓ of the nonuniformity. The corresponding solution of Eq. (3.3) has a soliton shape

$$W=1/\cosh^2(\zeta/\ell). \tag{3.7}$$

The uniform case corresponds to the limit $\ell\to\infty$, i.e., $\kappa\to1$, $W\to1$, which is also the case of incompressible flow. Thus, advection governed by Eqs. (3.4), (3.6), and (3.7) corresponds to the *CABC* flow, and we can observe changes of the advection pattern when the compressible flow approaches the incompressible limit by smooth change of the only parameter ℓ.

IV. RESULTS OF SIMULATIONS

It is worthwhile to start a discussion of advection with the incompressible case described by the *ABC* model (3.5) with $W\equiv1$. For $\epsilon=0$, the dynamics of a particle in the (x,y) plane, $z=\text{const}$, is integrable and can be interpreted without any problems. The dynamics along the z axis is trivially obtained by integration of the right-hand side of the third equation in Eq. (3.5), where x,y are known functions of time. Applying $\epsilon\neq0$ we make the dynamics nontrivially three dimensional and, therefore, chaotic [8–10].

The Poincaré map of a number of trajectories is shown in Fig. 1. Points on the plane $z=0$ in Fig. 1 are obtained as the points of intersection of a trajectory with the plane $z=0$ of a unit cell: $x,y,z \bmod 2\pi$. Closed orbits correspond to invariant cylinders along z, while the chaotic zone near the destroyed saddles belongs to the only trajectory which performs a random walk along the stochastic web [10] bounded in the z direction. The stochastic web was introduced and investigated in [10] for the *ABC* flow and some other types of flow with symmetry and quasisymmetry. This web signifies a three-dimensional connected channel of finite measure along

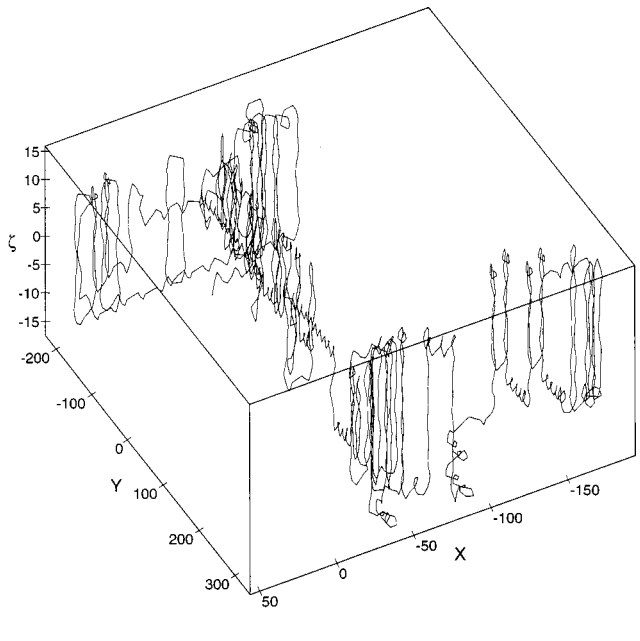

FIG. 2. Sample of trajectory for the *CABC* flow, with $\epsilon=0.9$, $\ell=12$.

which there exists three-dimensional mixing. The pattern is different in different planes of section $z=\text{const}$, which is why we do not see that the web is a connected net. It was also shown in [10] that the width δr of the web is

$$\delta r \sim \epsilon. \tag{4.1}$$

In Fig. 2 we present a typical trajectory in a slab geometry using the ζ variable instead of z. The trajectory is bounded in ζ. More detailed insight about trajectories comes from Fig. 3. The parameter ℓ provides a characteristic length scale of the nonuniformity of the helicity parameter $\kappa(z)$. One can consider $\ell\sim 1$ as a strong nonuniformity case. The corresponding Poincaré map of trajectories is given in Fig. 3 for system (3.4), with domain $x\in(-2\pi,2\pi)$; $y\in(-2\pi,2\pi)$; z $(-\infty,\infty)$, and a fairly large number of initial conditions. The phase portrait in the plane $z=0$ [Fig. 3(a)] displays invariant curves and domain of chaotic dynamics that covers the main part of the plane. Magnification of a fragment of the (x,y) plane is shown in Fig. 3(b) that demonstrates connectedness of different chaotic areas. The plane (ζ,x) is shown in Fig. 3(c) for $y=-\pi/2$. It is clearly seen that the dynamics along ζ (or along z) is bounded by invariant curves which makes the compressible case strongly different from the incompressible one. Upper and lower parts of the chaotic dynamics in Fig. 3(c) are not disjointed and their connection appears for different values of y [see Fig. 3(d)].

Comparing Fig. 3(a) to Fig. 1 we conclude that in spite of the small value of $\epsilon=0.05$, the area of chaotic dynamics increases in the compressible case. Even the decrease in ϵ in Fig. 4 does not sufficiently change the pattern, although the process of mixing slows down. In doing this comparison we mean the absence of big islands at *CABC* flow for small ϵ if one compares them to the sizes of islands for the *ABC* flow with the same ϵ. For a more adequate comparison, we need to consider a periodic dependence of $\kappa(z)$.

We can interpret the bounded dynamics along ζ in Fig. 3(c) by applying Arnold's theorem on the integrability of the advection to incompressible flow with $\kappa\neq\text{const}$. Level of compressibility can be measured by the derivative

$$c=\left|\frac{\ell\, d\ln[\kappa(\zeta)/\kappa(\infty)]}{d\zeta}\right|. \tag{4.2}$$

Consider the asymptotics $\zeta/\ell\to\infty$. Then from Eqs. (3.6) and (4.2) we have

$$c=O(\exp(-2\zeta/\ell)). \tag{4.3}$$

It follows from Eq. (4.3) that the compressibility is extremely small for $\zeta\gg\ell$, and one can expect integrable dynamics except for, maybe, exponentially narrow domains. The emergence of integrable solutions confines the dynamics along ζ as in Fig. 3(c).

The case of a large value of ℓ will be referred to as the adiabatic case. An example is given in Fig. 5. Surprisingly, it shows that almost all the area of motion belongs to the stochastic sea, and the size of islands becomes very small. In Fig. 5(b) we show a case of a much smaller value of $\epsilon=0.005$ with the same initial condition and the same computing time as in Fig. 5(a). Chaotic mixing covers the same area but slowly, more due to the smaller value of ϵ. Comparing Fig. 5 and Fig. 1, we conclude that compressibility enormously increases the mixing domain, especially in the adiabatic case. More precisely, for small ϵ the chaotic region in the *CABC* flow is of the order 1 in the (x,y) plane. On the other hand, the area of chaotic advection domain in the unit (x,y) cell of the *ABC* flow is of order ϵ.

V. ADVECTION IN A STRATIFIED FLOW

To understand the emergence of strong mixing in Fig. 5, let us consider the case of $\epsilon=0$. Equation (3.1) for the flow transforms into

$$v_x=-4\frac{dW}{d\zeta}\sin x-4W\sin y,$$

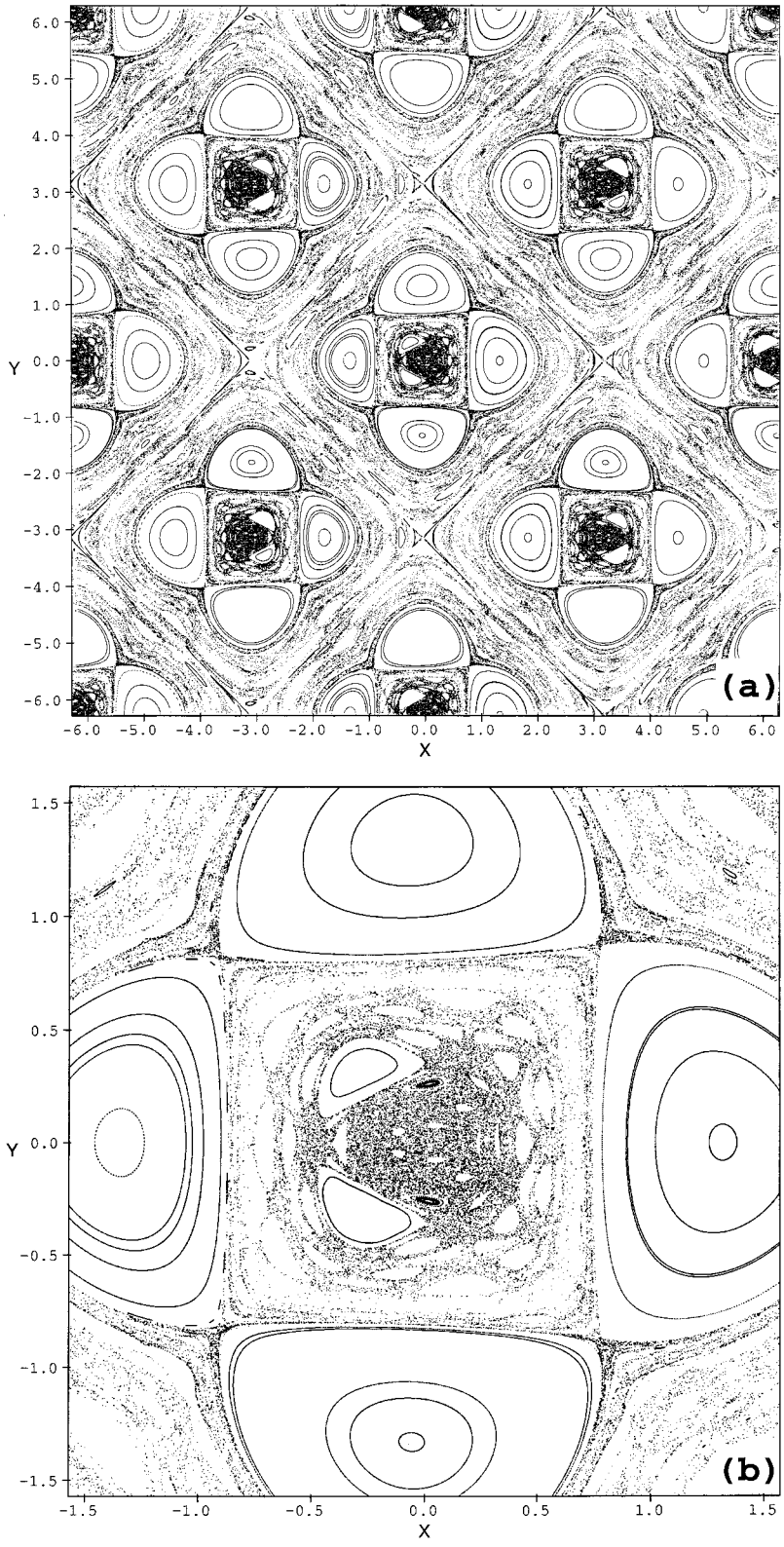

FIG. 3. Poincaré section of trajectories for the *CABC* flow with $\epsilon = 0.95$, $\ell = 1.1$. (a) A full cell in the (x,y) plane. (b) Magnification of the central part of (a). (c) The same in the (ζ,x) plane; $y = -\pi/2$. (d) The same in the (ζ,x) plane; $y = -\pi$.

$$v_y = -4\frac{dW}{d\zeta}\sin y + 4W\sin x,$$

$$v_z = 4\frac{W}{\kappa}(\cos x + \cos y), \tag{5.1}$$

which corresponds to a stratified flow along z. The corresponding incompressible case ($W = \text{const}$, $\kappa = 1$) gives a particular two-dimensional (2D) case of the *ABC* flow,

$$v_x = -4W\sin y,$$

$$v_y = 4W\sin x, \tag{5.2}$$

$$v_z = 4W(\cos x + \cos y).$$

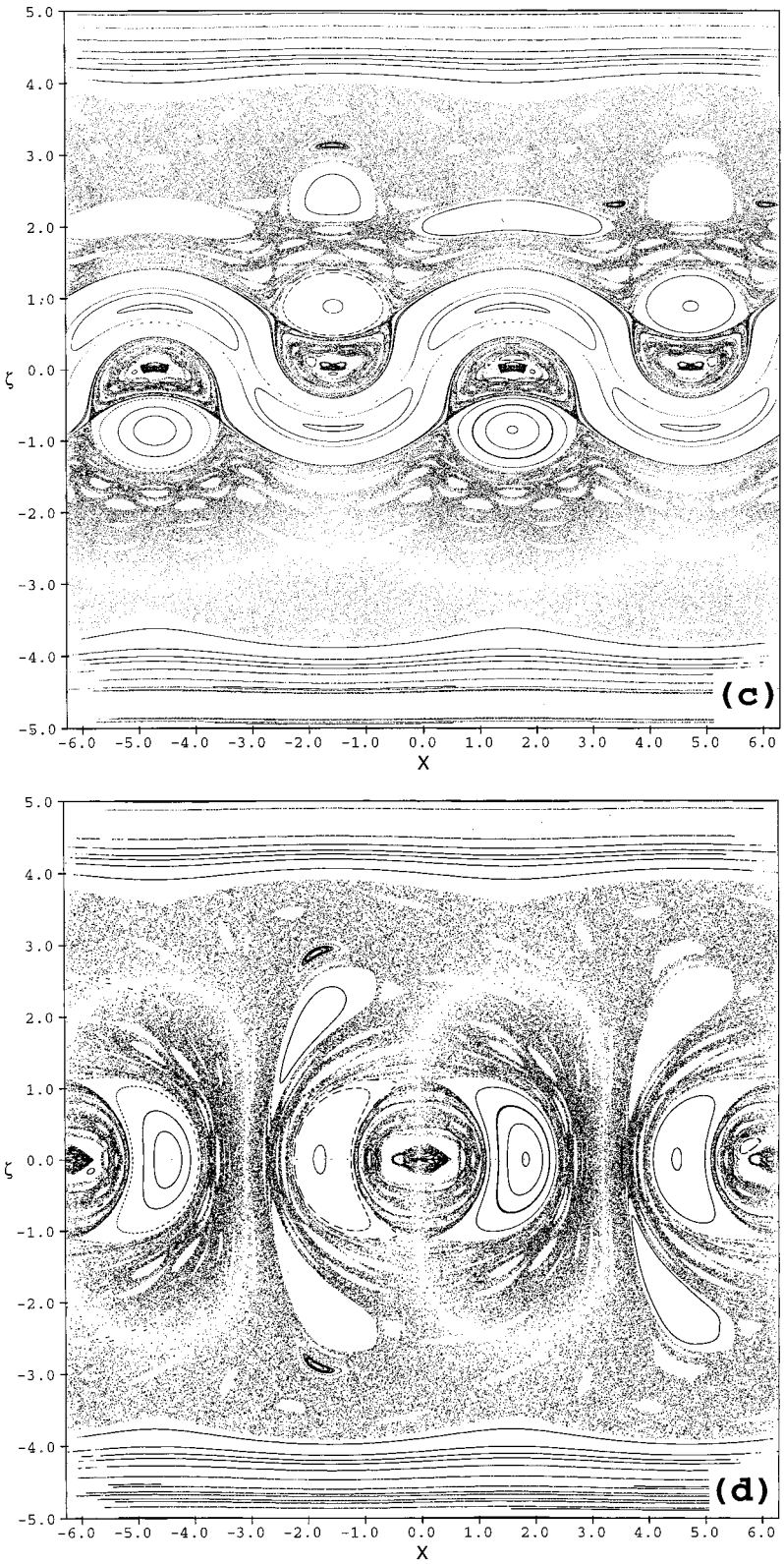

FIG. 3. (*Continued*).

Since the third equation is simply expressed through the first two equations, the corresponding advection equations

$$\dot{x} = -4W \sin y,$$

$$\dot{y} = 4W \sin x, \tag{5.3}$$

$$\dot{z} = 4W(\cos x + \cos y)$$

are trivially integrable.

In contrast to the incompressible *ABC* flow, the equations for the *CABC* advection for $\epsilon = 0$,

$$\dot{x} = -4\frac{dW}{d\zeta}\sin x - 4W \sin y,$$

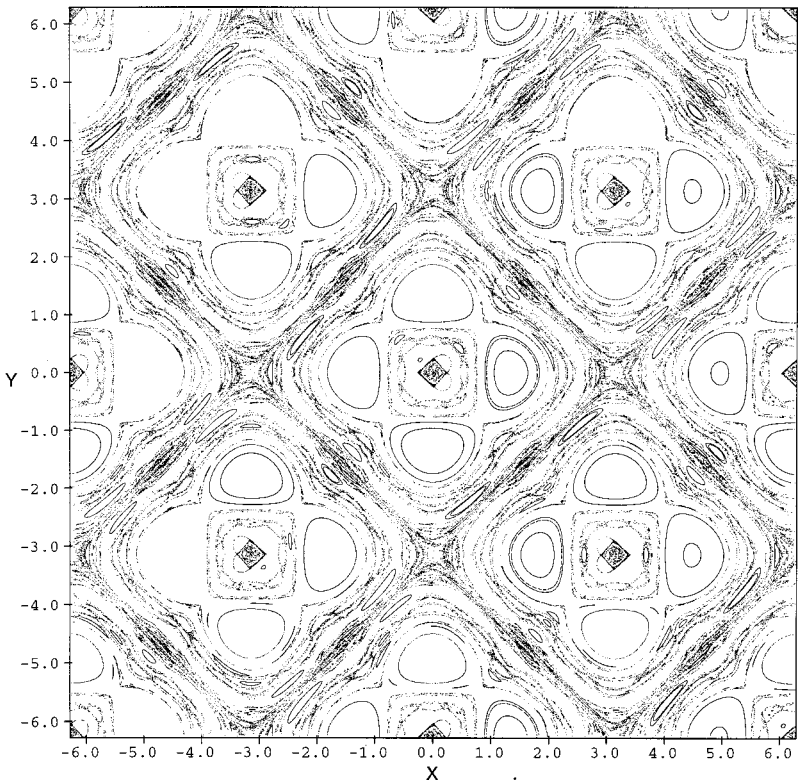

FIG. 4. Same as in Fig. 3(a) but for $\epsilon=0.005$, $\ell=1.1$.

$$\dot{y}=-4\frac{dW}{d\zeta}\sin y+4W\sin x,$$
$$\dot{z}=4\frac{W}{x}(\cos x+\cos y), \tag{5.4}$$

seem to be nonintegrable. Indeed, in deriving Eq. (5.4) we did not use any restriction on the dependence $\kappa=\kappa(z)$. In the case that $\kappa(z)$ is periodic on z, the same periodic property can be applied to $W(z)$ [compare to Eq. (3.3)]. Therefore the system (5.4) can be reduced to a typical Hamiltonian system with a periodic perturbation. Since the system with $W=$ const has a separatrix, we can immediately conclude the occurrence of stochastic layers of finite width for a periodic perturbation $W=W(z)$ [11]. Periodic perturbation with $W\neq$ const is a result of compressibility, i.e., $\kappa\neq$ const, and in this way compressibility increases the effective number of degrees of freedom of the system (5.4) from 1 to $1\frac{1}{2}$. In the case when $\kappa(z)$ is nonperiodic and smoothly localized along z [$\kappa(z)\to 0$ for $z\to\pm\infty$] the system is still with $1\frac{1}{2}$ degrees of freedom although it is not easy to prove the existence of chaos. We consider a numerical simulation of the problem for this situation. A Poincaré map corresponding to the system (5.4) in the plane $z=0$ for two values of $\ell=1.1$ and 20 is presented in Fig. 6. The plot in Fig. 6(a) shows many islands of different sizes. There are also many dots or short dashes. Magnification shows that all of them are, in fact, tiny narrow islands or island chains. The adiabatic case [Fig. 6(b)] has an even more drastic pattern where these narrow tiny islands are distributed fairly densely. We were unable to pick a chaotic trajectory, and any initial condition taken started a trajectory that belongs to a resonance set of islands. Actually, different islands of the same resonance chain should be separated by a stochastic layer which can be exponentially small and invisible.

To understand better the type of solutions of Eq. (5.4), we plot the periodic elliptic and hyperbolic points in Fig. 7, where we consider only cycles with periods (1–26) of crossings the plane $z=0$. The dense set of elliptic and hyperbolic points is in correspondence to the dense sets of island chains in Fig. 6. Even very small perturbation with $\epsilon\neq 0$ leads to an overlapping of the island chains and induces a global chaotic dynamics. The pattern of distribution of the stagnation points can explain increased mixing of the compressible flow, although we still need an explanation of why the islands are narrow and dense. It is worthwhile to mention that the case of the initial system (3.1) can include very narrow islands in addition to large ones, as it was found recently for the adiabatic case in [15] for a Hamiltonian model with $1\frac{1}{2}$ degrees of freedom.

VI. CONCLUDING REMARKS

Considering compressible generalization of the *ABC* flow we have come across an interesting phenomenon and an interesting dynamical system. We have observed much stronger global mixing properties than for the incompressible case. The mixing property prevails over almost the entire phase space, even for the small value of the parameter ϵ that comes with a dependence on the z coordinate. The area of chaotic dynamics is of order one, whereas for the *ABC* flow for the incompressible case the area of chaotic dynamics is of order ϵ. Thus, compressibility increases the mixing area in the (x,y) plane but makes the area bounded in z direction.

Since a Hamiltonian formulation of the advection in *CABC* flow is possible, the corresponding methods of analysis of Hamiltonian dynamics can be applied. For the consid-

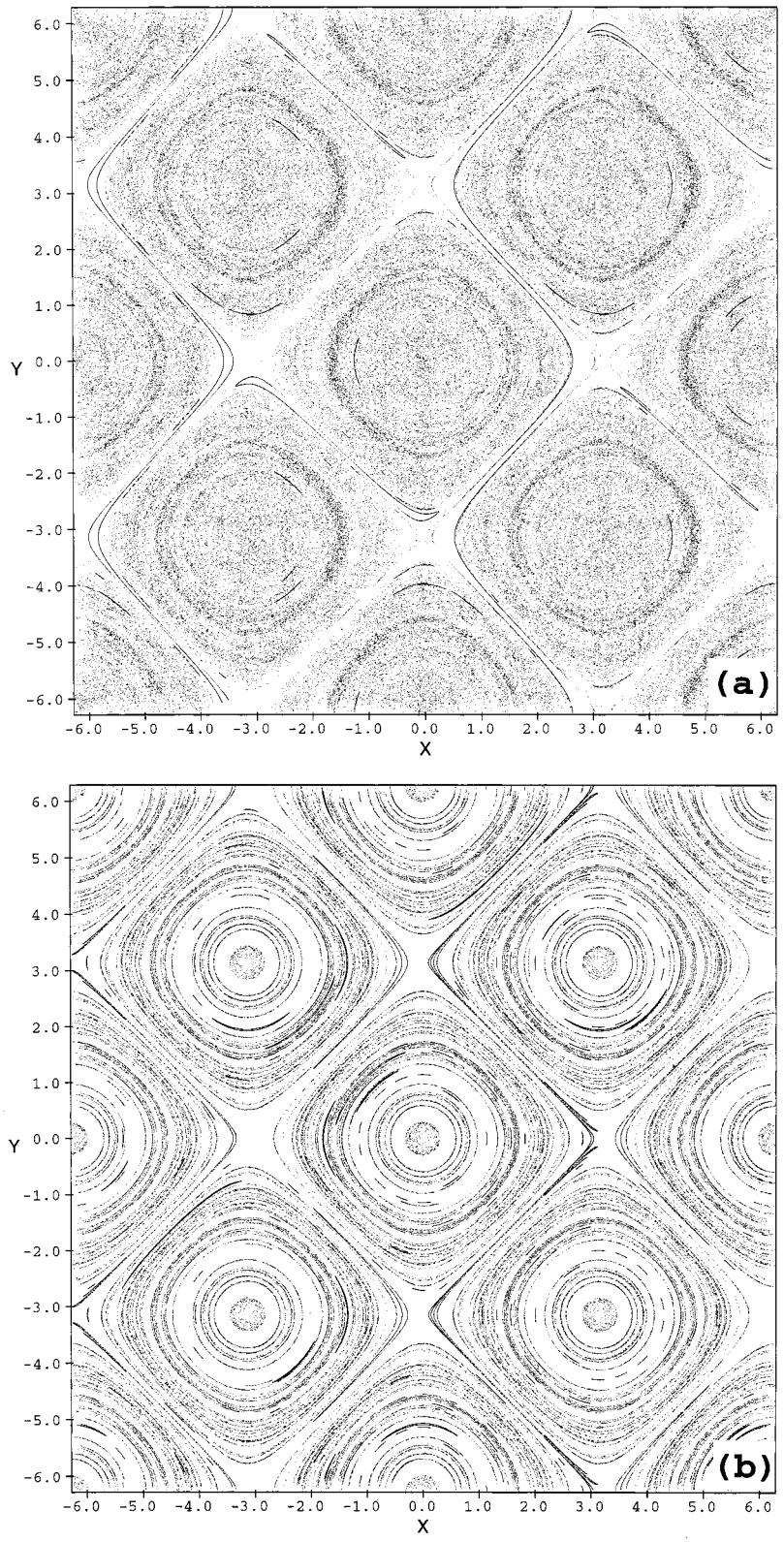

FIG. 5. Same as in Fig. 3(a) but for $\ell = 20$ and $\epsilon = 0.05$ (a), 0.005 (b). $\ell = 1.1$.

ered case, we encounter a new kind of a dynamical system with dense distribution of thin and tiny islands. Such a system is very sensitive to even small perturbations since the resonances can easily overlap as a result of the imposed perturbation. The last remark is related to the problem of a fast kinematic dynamo [4,6,16] (see also [17], and references therein). The problem is related to an exponentially growing magnetic field **B** that satisfies the equations

$$\frac{\partial \mathbf{B}}{\partial t} + \{\mathbf{v}, \mathbf{B}\} + \mathbf{B}\,\mathrm{div}\,\mathbf{v} = \frac{1}{R_m}\Delta \mathbf{B}, \tag{6.1}$$

where {,} denotes the Poisson bracket for two vector fields, and R_m is the magnetic Reynolds number. Mixing of the field lines of the vector field **v** is crucial for generating the magnetic field for the incompressible case $\mathrm{div}\,\mathbf{v} = 0$. In the

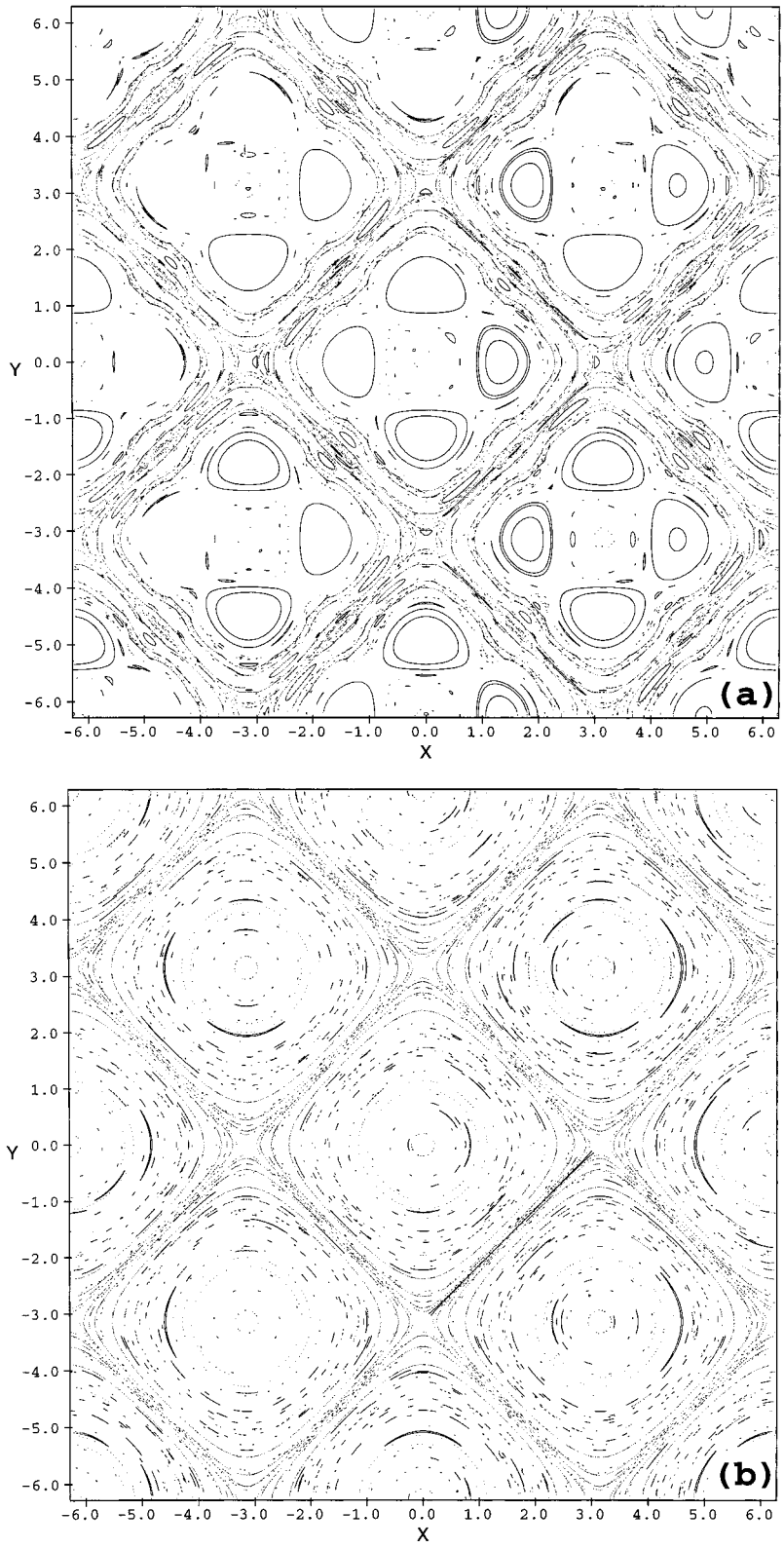

FIG. 6. Same as in Fig. 3(a) but for $\epsilon = 0$ and $\ell = 1.1$ (a), 20 (b).

compressible case of *CABC* flow we should speak about mixing of the advected particles rather than about field lines. The emergence of strong mixing with small characteristic scales can strongly influence the growth rate of **B**. The scale ℓ can be considered as a control parameter for the compressible situation. At the moment we cannot predict the magnetic field growth rate. On the one hand, we have a smaller scale of mixing and, on the other hand, we can observe from simulation the decreasing of the trajectory dispersion (Lyapunov exponents). We hope to discuss this problem in more detail in another paper. Here we only mention that compressibility may lead to a new interesting physics in magnetic field generation.

An important comment can be made for a force-free mag-

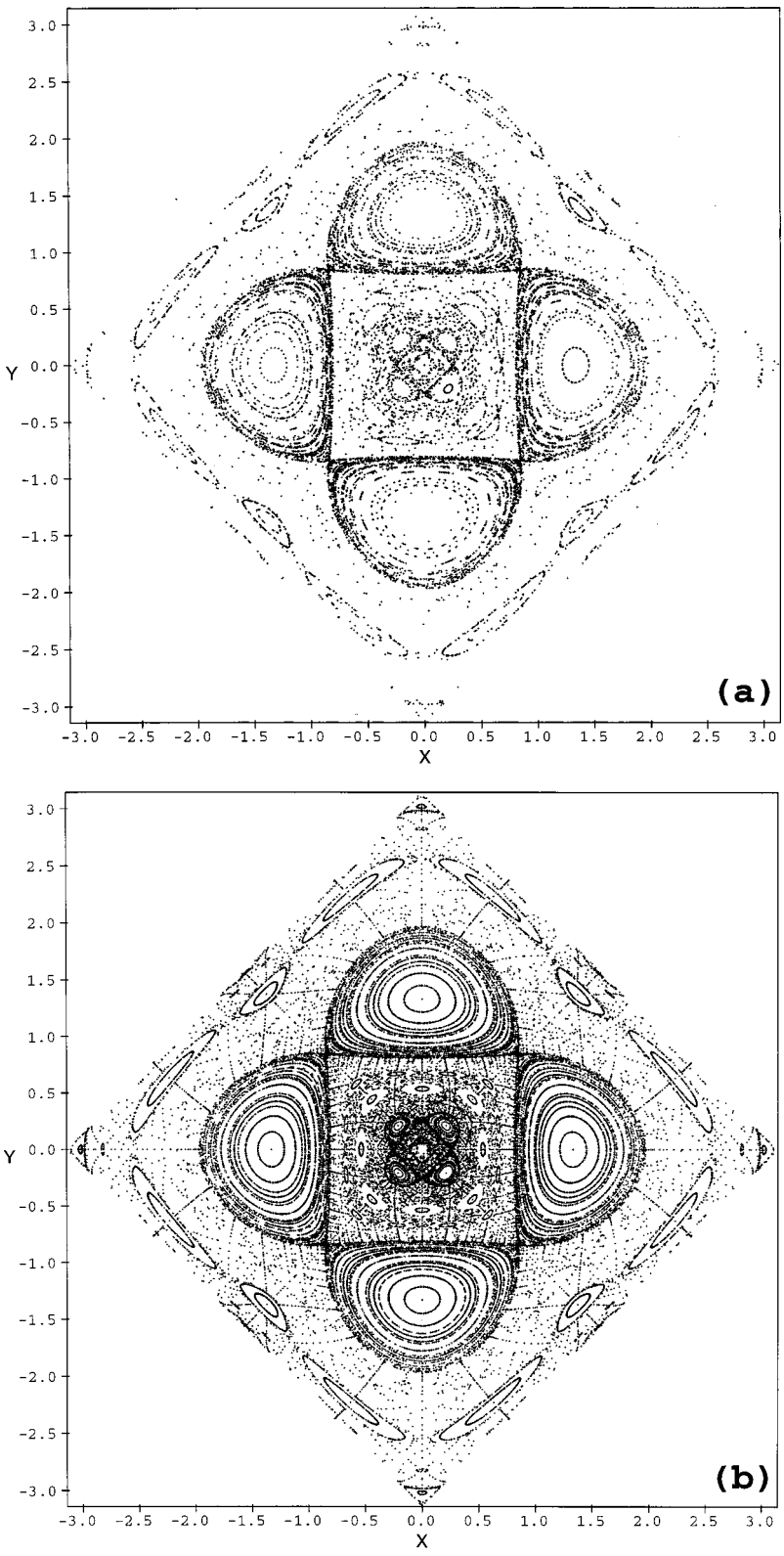

FIG. 7. Distributions of saddle points (a) and elliptic points (b) for the *CABC* flow with $\epsilon=0$, $\ell=1.1$ with a period within interval (1–26).

netic field which satisfies the same equation as Eq. (1.1),

$$\mathrm{curl}\mathbf{B}=\kappa\mathbf{B}. \tag{6.2}$$

In contrast to the velocity field **v**, we always have $\mathrm{div}\,\mathbf{B}=0$ and the case of $\kappa=\kappa(\mathbf{r})$ leads to the integrability of the equations for the magnetic field lines. Nevertheless, nontrivial situations for the magnetic field lines can occur when the vector fields **B** and **v** are coupled. An example of such solutions was recently proposed in [16].

ACKNOWLEDGMENTS

This work was supported by the U.S. Navy Department under Grant No. N00014-96-1-0055, and the U.S. Department of Energy under Grant No. DE-FG02-8692ER54184.

[1] V. I. Arnold, *Mathematical Methods of Classical Mechanics* (Springer, Berlin, 1989).
[2] V. I. Arnold and B. A. Khesin, *Topological Methods in Hydrodynamics* (Springer, Berlin, 1998).
[3] H. K. Moffatt, J. Fluid Mech. **159**, 359 (1985); **166**, 359 (1986).
[4] P. Constantin and A. Majda, Commun. Math. Phys. **115**, 435 (1988).
[5] V. I. Arnold and E. I. Korkina, Vestn. Mosk. Univ., Ser. 1: Mat, Mekh. **3**, 43 (1983).
[6] V. I. Arnold, C. R. Hebd. Seances Acad. Sci. **261**, 17 (1965).
[7] S. Childress, J. Math. Phys. **11**, 3063 (1970).
[8] M. Henon, C.R. Seances Acad. Sci., Ser. A **262**, 312 (1966).
[9] T. Dombre, U. Frisch, J. M. Greene, M. Henon, A. Mehr, and A. M. Soward, J. Fluid Mech. **167**, 353 (1986).
[10] G. M. Zaslavsky, R. Z. Sagdeev, and A. A. Chernikov, Zh. Eksp. Teor. Fiz. **94**, 102 (1988) [Sov. Phys. JETP **67**, 270 (1988)].
[11] G. M. Zaslavsky, R. Z. Sagdeev, D. A. Usikov, and A. A. Chernikov, *Weak Chaos and Quasiregular Patterns* (Cambridge University Press, Cambridge, England, 1991).
[12] A. A. Chernikov *et al.*, Phys. Lett. A **144**, 127 (1990).
[13] G. M. Zaslavsky, D. Stevens, and H. Weitzner, Phys. Rev. E **48**, 1683 (1993).
[14] A. Morgulis, V. I. Yudovich, and G. M. Zaslavsky, Commun. Pure Appl. Math. **XLVIII**, 571 (1995).
[15] A. I. Neishtadt, V. V. Sidorenko, and D. V. Treschev, Chaos **7**, 2 (1997).
[16] S. Childress, in *Topological Aspects of the Dynamics of Fluids and Plasmas*, edited by H. K. Moffatt, G. M. Zaslavsky, P. Compte, and M. Tabor (Kluwer, Dordrecht, 1992), pp. 111–148.
[17] S. M. Mahajan and Z. Yoshida, Phys. Rev. Lett. **81**, 4863 (1998).